An Analytical Approach to Estimate the Load-Bearing Capacity of Subgrade Soil with a Geocell-Reinforced Base Layer

Md. Ashrafuzzaman Khan, S.M.ASCE[1]; Anand J. Puppala, Ph.D., P.E., D.GE, F.ASCE[2]; Nripojyoti Biswas, S.M.ASCE[3]; Surya S. C. Congress, Ph.D., A.M.ASCE[4]; and Kamron H. Jafari, S.M.ASCE[5]

[1]Zachry Dept. of Civil and Environmental Engineering, Texas A&M Univ., College Station, TX. Email: mak2019@tamu.edu
[2]Zachry Dept. of Civil and Environmental Engineering, Texas A&M Univ., College Station, TX. Email: anandp@tamu.edu
[3]Zachry Dept. of Civil and Environmental Engineering, Texas A&M Univ., College Station, TX. Email: nripojyoti.biswas@tamu.edu
[4]Zachry Dept. of Civil and Environmental Engineering, Texas A&M Univ., College Station, TX. Email: congress@tamu.edu
[5]Zachry Dept. of Civil and Environmental Engineering, Texas A&M Univ., College Station, TX. Email: kjafari@tamu.edu

ABSTRACT

The widespread application of geocell can be attributed to its ability to provide additional confinement to the infill material and increase the load-bearing capacity. There are limited analytical approaches available to calculate the bearing capacity of the geocell-reinforced foundation. The available methods consider the lateral earth pressure theory, which may lead to the underestimation (active condition) or overestimation (at rest condition) of the bearing capacity values. This paper presents an analytical approach to calculate the improvement in load-bearing capacity of pavement foundation systems reinforced with geocell in the base layer. The proposed method estimated the radial stresses within the base layer from the theory of elasticity, which can be used to determine the bearing capacity of the unpaved road section. The proposed method yielded the most accurate results when the applied stress was within 50% of the ultimate stress.

INTRODUCTION

Construction of pavements over poor subgrade is a major cause of concern for pavement engineers and contractors (Mandal and Gupta 1994, Punthutaecha et al. 2006, Puppala et al. 2008, 2017, Chakraborty et al. 2020). Several techniques, including piled embankment, ground improvement with chemicals, geosynthetics reinforcements, are some of the available methods to improve the load-carrying capacity of the subgrade soil (Almeida et al. 2015, Neto et al. 2015, Satvati et al. 2020, Alimohammadi et al. 2021, Biswas et al. 2021b). High-strength planar geosynthetic such as geogrid and geotextile can be used in pavement layers to reduce the stresses at the top of the subgrade (Kwon et al. 2005, Zornberg et al. 2008, Biswas et al. 2021a, 2021b). However, the planar confinement fails to restrain the overall movement of the base layer, especially in the case of poor-quality aggregates (Han et al. 2013). Alternatively, Geocells could provide three-dimensional confinement to the infill material and subsequently reduce the stresses at the top of the subgrade (Sireesh et al. 2009, Han et al. 2013, George et al. 2019, Khan et al. 2022).

Geocells are made from High-Density Poly-Ethylene (HDPE) sheets used to retrain lateral movements in the infill material (George et al. 2019, Khan et al. 2020a, 2020b). Several researchers have conducted laboratory and field studies on geocell-reinforced pavements to understand the load-transfer mechanism and quantify the improvement in pavement performance (Thakur et al. 2012; Suku et al. 2016). The vertical load-bearing capacity increases with an increase in the geocell pocket diameter to loading plate ratio and the aspect ratio of the geocell (Mhaiskar and Mandal 1996). A number of laboratory studies are currently available to determine the bearing capacity improvement factor for the geocell-reinforced system (Rajagopal et al. 2014, Dash et al. 2019).

Limited analytical studies are available to interpret the bearing capacity of the geocell-reinforced soil by considering the effect of confinement (Koerner 2005, Presto 2008, Zhang et al. 2010, Avesani Neto et al. 2013, Hegde and Sitharam 2015). The previous methods considered either active earth pressure or earth pressure at rest theory to determine the lateral stresses acting on the geocell location, which were not able to capture the actual stress transferred to the geocell wall. In this study, a bearing capacity calculation method was proposed for geomaterial reinforced with geocell by realistic consideration of the vertical and horizontal distributions of stresses derived from Boussinesq's solution. A prediction model was developed based on these stress estimations. This model was validated by comparing its prediction with experimental measurements. The paper presents an overview of this model and its prediction assessments.

The proposed method can predict the bearing capacity for the geocell reinforced sections with better accuracy. This approach can be used to determine the required thickness of the base layer of an unpaved road.

BACKGROUND

Several bearing capacity calculation methods are available to consider the improvement provided by the geocell reinforcement (Koerner 2005, Presto 2008, Avesani Neto et al. 2013). These bearing capacity equations can be represented by the following Eq. 1.

$$q_r = q_u + \lambda q \tag{1}$$

Where the ultimate bearing capacity of the reinforced section (q_r) is equal to the summation of the ultimate bearing capacity of the unreinforced subgrade bearing capacity (q_u) and the product of the applied vertical stress (q) and the improvement factor (λ) due to reinforcements. The λ value depends on the dissipation of stresses due to the geocell reinforced base layer. Table 1 summarizes the previous methods used to determine the improvement factor (λ) for the geocell reinforced base layer. The pre-existing methods are primarily based on earth pressure theory. However, the flexible pavement system is analyzed as a layered elastic system; therefore, a novel elasticity-based approach was introduced in this study to estimate the bearing capacity of the pavement foundation system.

PROPOSED BEARING CAPACITY PREDICTION METHOD

The following sections present the methodology adopted in this study to develop the analytical approach. The flowchart shown in Figure 1a describes the steps involved in determining the proposed equation. Figure 1b shows the geometry and loading conditions adopted for the development of the proposed method.

Table 1. Existing methods for calculating improvement factor (λ)

Method	Improvement factor (λ)	Description
Koerner (2005)	$2k_a tan\delta$	k_a = active earth pressure coefficient, δ = interface friction angle
Presto (2008)	$(2\frac{h}{d}k_a tan\delta)I$	I = the average stress influence factor based on Boussinesq's solution
Avesani Neto et al.'s (2013)	$(1 + 4e\frac{h}{d}k_o tan\delta - e)$ $e = \frac{BL}{(B+2d)(L+2d)}$	k_o = earth pressure coefficient at rest, d = diameter of the geocell e = load dissipation angle B, L = width and length of the footing

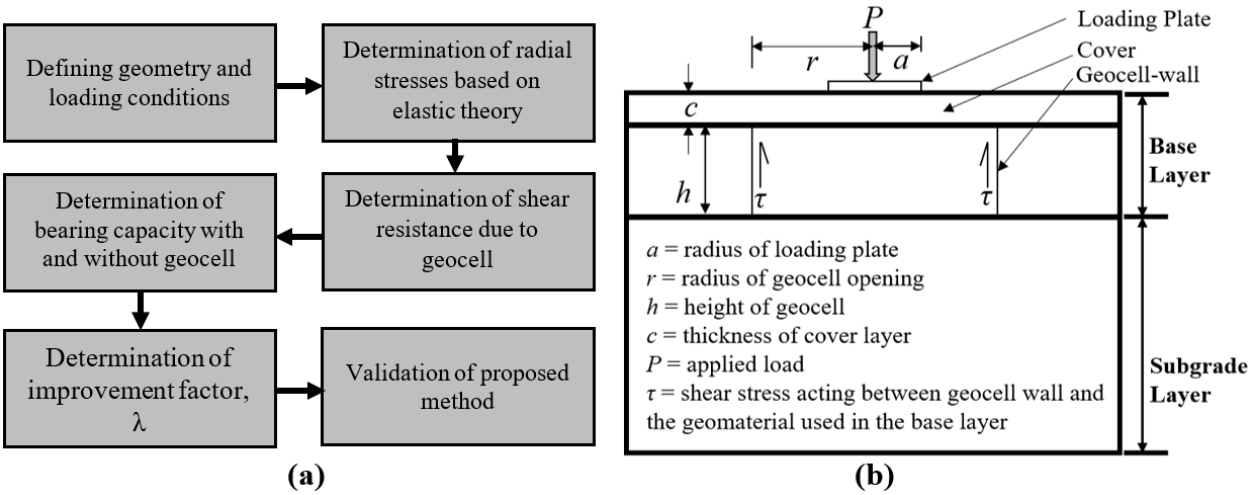

Figure 1. Development of the proposed method: a) flowchart of the research methodology; b) geometry and loading conditions

Geometry and loading conditions. In this study, a static load test (Figure 1b) was considered to compare the proposed method with existing methods. A three-layer system was considered with subgrade soil located at the bottom, a geocell reinforced base layer at the middle and a thin cover layer at the top. The load (P) is applied at the top of the steel plate of radius 'a', which is placed just above the cover layer. The radius of the opening of the geocell is 'r' (where $r = d/2$, d = diameter of geocell pocket), and the centerline of the load plate is aligned with the centerline of the geocell. When the vertical load is applied, an increase in horizontal stress will generate additional pressure on the geocell walls. It was assumed that the horizontal stress would be equal to the confining stress offered by the geocell; consequently, there will be an increase in the acting shear stress between infill material and geocell wall.

Determination of radial stress. Geocells provide radial confinement for the infill material, which depends on the type of infill material, stiffness and geometry of the geocell, and vertical stress (q) applied at the top of the geocell layer. In this study, radial stress (σ_r), acting at the mid-depth ($z = c + 0.5h$) of the base layer was calculated based on the elastic theory (Eq. 2).

$$\sigma_r = q\,[2\mu A + C + (1\text{-}2\mu)F] \quad (2)$$

where, μ = Poisson's ratio of the infill material; c = thickness of the cover layer.

A, C, and F are the stress influence factors that depend on the (z/a) and (r/a) ratios.

The value of horizontal stress increment is a function of the applied load, Poisson's ratio of the infill material, radius of the load plate (a), the radius of the geocell opening area (r), and the depth (z) from the bottom of the loading plate. Based on the geometry (z/a, r/a), influence factors for vertical and radial stresses can be calculated using the set of graphs shown in Figure 2. These graphs were reproduced from the tabulated results reported by Ahlvin and Ulery (1962).

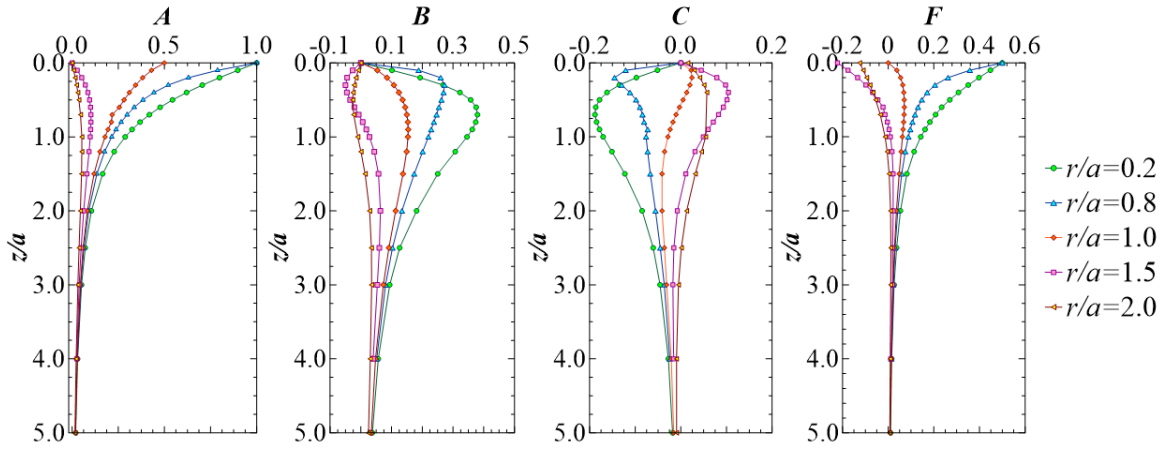

Figure 2. Stress influence factors

Determination of the shear resistance due to geocell. A portion of the applied load will be resisted by the shear stresses acting between the geocell-geomaterial interface. The resisting shear stress (τ) and shear force (S) can be calculated using Eq. 3 and 4, respectively.

$$\tau = tan(\delta)\sigma_r \tag{3}$$

$$S = 2\pi rh.tan(\delta)\sigma_r \tag{4}$$

Determination of improvement due to stress distribution. Vertical stresses acting at the top of the geocell (q) is higher as compared to the stresses acting at the bottom (q'), i.e., at the top of the subgrade layer. Load acting at the top of subgrade soil will be reduced due to the shear resistance provided by the geocell-geomaterial interface as well as due to the distribution of the vertical stresses over a wider area. Using Boussinesq's solution, the value of q' could be correlated to actual stresses on top of the geocell and the shear stress developed due to geocell confinement Eq. 5.

$$q'\pi r^2 = q(A + B)\pi r^2 - 2\pi rh.tan(\delta)\sigma_r \tag{5}$$

Here, A and B are vertical stress influence factors, which can be determined from Figure 2. Therefore, the effective vertical stress acting on the bottom of the geocell can be represented by Eq. 6 or Eq. 7.

$$q' = q(A + B) - \frac{2h.tan(\delta)\sigma_r}{r} \tag{6}$$

$$q' = q(A + B) - \frac{4h.\tan(\delta)\sigma_r}{d} \quad (7)$$

Bearing capacity of the unreinforced and reinforced sections. Bearing capacity for unreinforced soil was determined using Terzaghi's method (Eq. 8).

$$q_u = cN_cS_c + \frac{1}{2}\gamma BN_\gamma S_\gamma \quad (8)$$

Where, q_u = unreinforced subgrade bearing capacity;
c = cohesion of the subgrade soil;
N_c, N_γ = bearing capacity factor;
S_c = 1.3 for circular and rectangular loads, 1.0 for strip loads;
S_γ = 0.6 for circular load, 0.8 for rectangular loads and 1.0 for strip loads.

The improvement due to the geocell layer can be calculated by the difference in applied stresses at the top and the bottom of the reinforced layer. The following set of equations (Eqs. 9-13) can be used to determine the capacity of the reinforced section.

$$q_r = q_u + (q - q') \quad (9)$$

$$q_r = q_u + q\{1 - (A + B)\} + \sigma_r \frac{4h.\tan(\delta)}{d} \quad (10)$$

$$q_r = q_u + q\left[\{1 - (A + B)\} + [2\mu A + C + (1 - 2\mu)F]\frac{4h.\tan(\delta)}{d}\right] \quad (11)$$

$$q_r = q_u + \lambda q \quad (12)$$

$$\lambda = [1 - (A + B)] + [2\mu A + C + (1 - 2\mu)F]\frac{4h.\tan(\delta)}{d} \quad (13)$$

The improvement factor (λ) depends on the infill material property (μ), geocell-geomaterial interface friction angle (δ), geocell geometry (d, h), and stress influence factors (A, B, C, and F). In the following section, λ-values obtained from different pre-existing methods and the proposed method were compared using the results from an experimental study conducted by Menses (2004).

VALIDATION OF THE PROPOSED METHOD

Stress dissipation. Laboratory test results on geocell reinforced soil, presented by Meneses (2004), were used to validate, and compare the proposed improvement factor (Table 2). The tests were performed on clay subgrade with cohesion of 20 kPa, and sand with a friction angle of 35° was used to fill the geocell pockets. The vertical load was applied with a circular plate of radius, a = 175 mm, and tests were performed for different aspect ratios (h/d = 0.26, 0.52, 0.78) of HDPE geocells. Table 2 shows the load improvement due to geocell reinforcement (h/d = 0.26; height, h = 50 mm and pocket size, d = 190 mm) obtained from experimental results and predicted from different methods.

Table 2. Comparison of improvement factor, λ computed using different analytical methods with experimental results of Meneses (2004) with h/d = 0.26

Applied Load, *P* (kN) / Methods	31.2	62.4	93.5	124.7	155.9	187.1
Experimental results from Meneses (2004)	0.52	0.58	0.65	0.71	0.76	0.75
Koerner's method (M1)	0.18	0.18	0.18	0.18	0.18	0.18
Presto's method (M2)	0.06	0.06	0.06	0.06	0.06	0.06
Avesani Neto et al.'s method (M3)	0.83	0.81	0.81	0.81	0.81	0.81
Proposed method (M4)	0.61	0.61	0.61	0.61	0.61	0.61

The improvement factors computed from Koerner's (M1) and Presto's (M2) methods were around 24-35% and 8-11% of the measured values, respectively. This is attributed to the consideration of active earth pressure conditions in stress calculations, leading to a lower stress transfer to the geocell wall. At a lower level of stress, the calculated load carrying capacities from Avesani Neto et al. (M3) and proposed (M4) methods were 59% and 17% higher, respectively. At the ultimate stress level, the predicted improvement factors from M3 were 8% higher, whereas the predicted values from M4 were 19% lower. M3 overestimated the load-carrying capacity due to the consideration of earth pressure at rest conditions. It could be noted that M4 predicted better λ-values as compared to other methods due to the consideration of the radial stresses from the theory of elasticity.

Comparisons between theoretical and experimental stress dissipations for geocells with three different aspect ratios (h/d = 0.26, 0.52, and 0.78) are shown in Figures 3a-3c. The stress dissipation (q_d) was calculated from the difference of applied stress on top of the geocell layer and the stress acting at the bottom of the geocell layer. The performance of different analytical approaches was measured in terms of the ratio of the predicted ($q_{d\text{-}predicted}$) and measured ($q_{d\text{-}experimetnal}$) values of stress dissipation for three different stress levels (25%, 50%, and 100% of the ultimate stress). It can be observed that both M1 and M2 methods underpredicted the reduction of stress due to geocell, whereas M3 overpredicted the bearing capacity with geocell. The prediction of q_d value from the proposed method (M4) was close to the experimental value when the ratio of the applied stress to the ultimate stress was around 0.50, and h/d ratio was 0.26. Furthermore, M4 also provides a better fit with the experimental results when compared to M3 for different aspect ratios of the geocell (Figure 3).

The M3 assumed earth pressure at rest condition (k_o), which indicates the ratio of horizontal to vertical stress will be 0.43, whereas the active earth pressure coefficient (k_a) value is 0.27. In addition to the shear resistance computed from the lateral stress, M3 methods also consider the stress distribution factor, which results in the overestimation of the bearing capacity. The at-rest earth pressure condition does not consider any movement of the geocell wall. However, this assumption may lead to ambiguity regarding the stress transfer mechanism since the geocell walls are not rigid and may undergo movements.

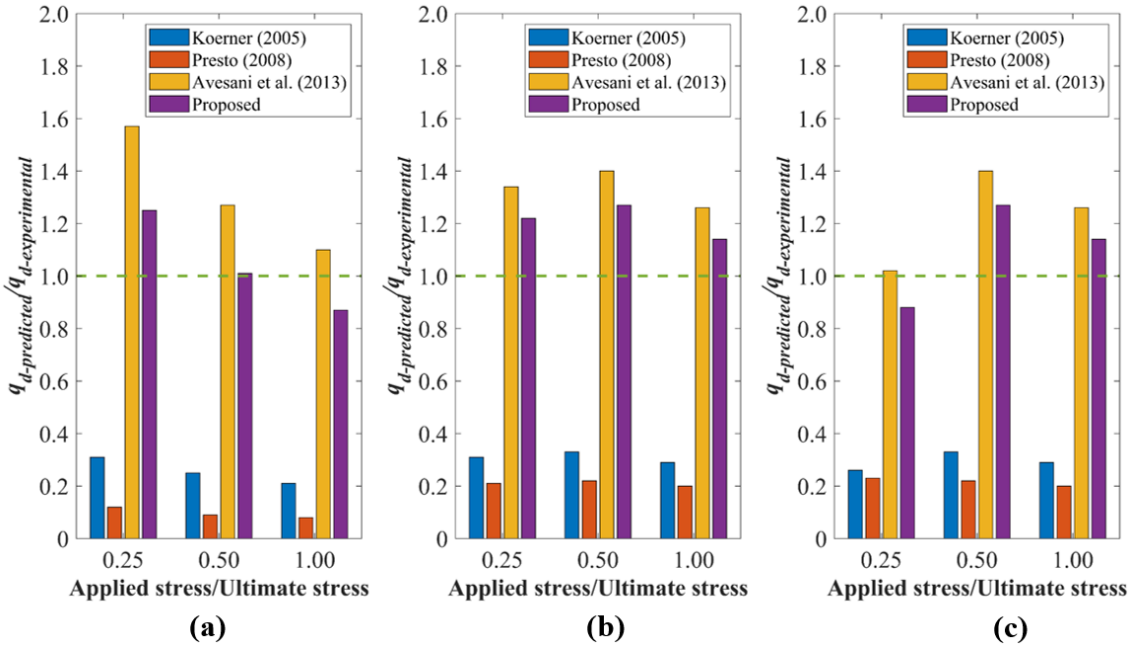

Figure 3. Performance of proposed and existing analytical approaches based on experimental results reported by Meneses (2004) for geocell having aspect ratio of (a) h/d = 0.26; (b) h/d = 0.52; (c) h/d = 0.78

Effect of geocell stiffness. The proposed and existing analytical approaches did not consider the effect of the stiffness of the geocell layer, as it was considered as a very high strength material to withstand the load transferred to it. However, the minimum required value of geocell stiffness (M) can be calculated from Eq. 14, which assumes that the additional confinement offered by the geocell is equal to the amount of radial stress transfer to the geocell wall. This equation is based on the membrane theory of Henkel and Gilbert (1952). This is applicable for undrained loading conditions, where the ratio of horizontal to vertical strain within the base layer is approximately 0.553 times and the Poisson's ratio, $\mu = 0.5$.

$$M = qr[A + C\,]\,\frac{1-\varepsilon_a}{0.553*\varepsilon_a} \tag{14}$$

Consider a 15 cm thick base layer with a 2.5 cm cover layer, which is constructed over the subgrade soil. The stress applied on top of the geocell layer is q = 187 kPa. The radius of the geocell (r) is 15 cm (6 inches), and the radius of the loading plate (a) is 15 cm. The stress influence factors A & C can be determined from Figure 2. At the ultimate stage of loading, if the vertical strain (ϵ_a) is around 0.11, the minimum required geocell stiffness will be 18.2 kN/m, according to Eq. 14. The vertical strain observed from the static load testing corresponding to the ultimate capacities varied from 0.08 to 0.14 (Meneses 2004); hence, the average vertical strain of 0.11 was considered in this example. Equation 14 can be to determine the minimum required stiffness for the geocells for the foundation system with different bearing capacities. Overall, using the proposed bearing capacity equation and the minimum required stiffness of the geocell, pavement foundation systems could be designed with an elastic approach, based on realistic stress values.

CONCLUSIONS

In this study, an analytical approach was proposed to calculate the bearing capacity of a geocell reinforced section. This analytical approach was compared with the existing bearing capacity methods and available experimental results to compute the improvement offered by the geocell. The proposed bearing capacity equation can be used to determine the required thickness of the base layer of unpaved road sections. The following conclusions can be drawn based on the current study and analyses of results presented in this paper:

- The proposed method is suitable for determining the bearing capacity of unpaved roads.
- The improvement factor, λ, depends on the location and aspect ratio of the geocell.
- λ value increases with the increase in the height to depth ratio (h/d) of geocell.
- The proposed method could accurately predict the additional load carrying capacity when the applied stress to ultimate stress ratio is around 0.50.
- At the ultimate stage of loading, the proposed method slightly underestimates the load-bearing capacity; however, the overall performance is better than the available analytical methods.

For future studies, the reduction of vertical stresses obtained from the proposed method could be utilized to develop design charts for unpaved roads. These design charts will be helpful for the transportation agencies to select the thickness of the geocell-reinforced base layers.

ACKNOWLEDGEMENTS

This research was funded by Industrial Fabrics, Inc. (Mr. Jay Richardson, Mr. Cody Colvin, and Mr. Al Florez). The authors also acknowledge the support of the NSF Industry-University Cooperative Research Center (I/UCRC) program funded 'Center for Integration of Composites into Infrastructure (CICI)' site at TAMU (NSF PD: Dr. Prakash Balan; Award #2017796)

REFERENCES

Ahlvin, R. G., and Ulery, H. H. (1962). "Tabulated Values for Determining the Complete of Pattern of Stresses, Strains, and Deflections Beneath a Uniform Circular Load on a Homogeneous Half Space". *Highway Research Board Bulletin*, 342, 1–13.

Alimohammadi, H., Zheng, J., Schaefer, V. R., Siekmeier, J., and Velasquez, R. (2020). "Evaluation of geogrid reinforcement of flexible pavement performance: A review of large-scale laboratory studies". *Transp. Geotech.*, 27, 100471(1-11).

Almeida, M. S. S., Hosseinpour, I., Riccio, M., and Alexiew, D. (2015). "Behavior of Geotextile-Encased Granular Columns Supporting Test Embankment on Soft Deposit". *J. Geotech. Geoenviron. Eng.* 141(3): 1–9.

Avesani Neto, J. O., Bueno, B. S., and Futai, M. M. (2013). "A bearing capacity calculation method for soil reinforced with a geocell". *Geosynth. Int.*, 20(3), 129–142.

Biswas, N., Puppala, A. J., Khan, M. A., Chakraborty, S., and Congress, S. S. C. (2021a). "Depth of Influence of a Wicking Geotextile below the Flexible Pavement Constructed over Expansive Subgrade". In *Geosynthetics Conference*, 583–594.

Biswas, N., Puppala, A. J., Khan, M. A., Congress, S. S. C., Banerjee, A., and Chakraborty, S. (2021b). "Evaluating the Performance of Wicking Geotextile in Providing Drainage for Flexible Pavements Built over Expansive Soils". *Transp. Res. Rec.*

Chakraborty, S., Puppala, A. J., and Biswas, N. (2020). "Role of crystalline silica admixture in mitigating ettringite-induced heave in lime-treated sulfate-rich soils". *Géotechnique*,: 1–17.
Dash, S. K., Saikia, R., and Nimbalkar, S. (2019). "Contact Pressure Distribution on Subgrade Soil Underlying Geocell Reinforced Foundation Beds". *Frontiers in Built Environment.*
George, A. M., Banerjee, A., Puppala, A. J., and Saladhi, M. (2019). "Performance evaluation of geocell-reinforced reclaimed asphalt pavement (RAP) bases in flexible pavements". *Int. J. Pavement Eng.*, 1–11.
Han, J., Thakur, J. K., Parsons, R. L., Pokharel, S. K., Leshchinsky, D., and Yang, X. (2013). "A summary of research on geocell-reinforced base courses". In *Design and Practice of Geosynthetic-Reinforced Soil Structures*. Edited by H.J. and T.F. Ling, H., Gottardi, G., and Cazzuffi, D. Bologna., 331–340.
Hegde, A., and Sitharam, T. G. (2015). "Experimental and analytical studies on soft clay beds reinforced with bamboo cells and geocells". *Int. J. Geosynth. Ground Eng.*, 1(2), 1-11.
Henlkel, J., and Gilbert, D. (1952). "The Effect Measured of the Rubber Membrane on the Triaxial Compression Strength of Clay Samples". *Géotechnique*, 3(1): 20–29.
Khan, M. A., Biswas, N., Banerjee, A., Congress, S. S. C., and Puppala, A. J. (2022). "Effectiveness of Double-Layer HDPE Geocell System to Reinforce Reclaimed Asphalt Pavement (RAP)-Base Layer". In *Advances in Transportation Geotechnics IV*. Springer, Cham., 593-604.
Khan, M. A., Biswas, N., Banerjee, A., and Puppala, A. J. (2020a). "Field performance of geocell reinforced recycled asphalt pavement base layer". *Transp. Res. Rec*, 2674(3), 69–80.
Khan, M. A., Nripojyoti, B., Banerjee, A., and Puppala, A. J. (2020b). "Performance of Geocell-Reinforced Recycled Asphalt Pavement (RAP) Bases in Flexible Pavements Built on Expansive Soils". In *Geo-Congress 2020*. American Society of Civil Engineers, Reston, VA., 488–497.
Koerner, R. M. (2005). *Desining with Geosynthetics*. In Fifth Edit. Pearson Prentice Hall.
Kwon, J., Tutumluer, E., and Kim, M. (2005). "Development of a mechanistic model for geosynthetic-reinforced flexible pavements". *Geosynth. Int.* 12(6), 310–320.
Mandal, J. N., and Gupta, P. (1994). "Stability of geocell-reinforced soil". *Constr. Build. Mater.*, 8(1): 55–62.
Mhaiskar, S. Y., and Mandal, J. N. (1996). "Investigations on soft clay subgrade strengthening using geocells". *Constr. Build. Mater.*, 10(4), 281–286.
Neto, J. O. A., Bueno, B. S., and Futai, M. M. (2015). "Evaluation of a calculation method for embankments reinforced with geocells over soft soils using finite-element analysis". *Geosynth. Int.*, 22(6), 439-451.
Presto. (2008). *GEOWEB load support overview*. Appleton, WI.
Punthutaecha, K., Puppala, A. J., Vanapalli, S. K., and Inyang, H. (2006). "Volume Change Behaviors of Expansive Soils Stabilized with Recycled Ashes and Fibers". *J. Mater. Civ. Eng.*, 18(2): 295–306.
Puppala, A., Hoyos, L., Viyanant, C., and Musenda, C. (2008). "Fiber and Fly Ash Stabilization Methods to Treat Soft Expansive Soils". In *Soft ground technology*, 136-145.
Puppala, A. J., Pedarla, A., Chittoori, B., Ganne, V. K., Nazarian, S., Puppala, A. J., and Pedarla, A. (2017). "Long-Term Durability Studies on Chemically Treated Reclaimed Asphalt Pavement Material as a Base Layer for Pavements". *Transp. Res. Rec*, 2657, 1–9.
Rajagopal, K., Chandramouli, S., Parayil, A., and Iniyan, K. (2014). "Studies on geosynthetic-reinforced road pavement structures". *Int. J. Geotech. Eng.*, 8(3), 287–298.

Satvati, S., Alimohammadi, H., Rowshanzamir, M., and Hejazi, S. M. (2020). "Bearing Capacity of Shallow Footings Reinforced with Braid and Geogrid Adjacent to Soil Slope". *Int. J. Geosynth. Ground Eng.*, 6(4), 1–12.

Sireesh, S., Sitharam, T. G., and Dash, S. K. (2009). "Bearing capacity of circular footing on geocell–sand mattress overlying clay bed with void". *Geotextiles and Geomembranes*, 27(2), 89–98.

Suku, L., Prabhu, S. S., Ramesh, P., and Babu, G. L. S. (2016). "Behavior of geocell-reinforced granular base under repeated loading". *Transp. Geotech.*, 9(2016), 17–30.

Thakur, J. K., Han, J., Pokharel, S. K., and Parsons, R. L. (2012). "Performance of geocell-reinforced recycled asphalt pavement (RAP) bases over weak subgrade under cyclic plate loading". *Geotextiles and Geomembranes*, 35, 14–24.

Zhang, L., Zhao, M., Shi, C., and Zhao, H. (2010). "Bearing capacity of geocell reinforcement in embankment engineering". *Geotextiles and Geomembranes*, 28(5), 475–482.

Zornberg, J. G., Prozzi, J. A., Gupta, R., Luo, R., McCartney, J. S., Ferreira, J. Z., and Nogueira, C. (2008). "Validating Mechanisms in Geosynthetic Reinforced Pavements". FHWA/TX-08/0-4829-1, Center for Transportation Research (CTR), Austin.